

Available online at [www.sciencedirect.com](http://www.sciencedirect.com)

ScienceDirect

[www.elsevier.com/locate/jes](http://www.elsevier.com/locate/jes)**JES**  
JOURNAL OF  
ENVIRONMENTAL  
SCIENCES  
[www.jesc.ac.cn](http://www.jesc.ac.cn)

## Process analysis of PM<sub>2.5</sub> pollution events in a coastal city of China using CMAQ

Qiang Zhang<sup>1</sup>, Di Xue<sup>1</sup>, Xiaohuan Liu<sup>1,2,3,\*</sup>, Xiang Gong<sup>4</sup>, Huiwang Gao<sup>1,2,3</sup>

1. College of Environmental Science and Engineering, Ocean University of China, Qingdao 266100, China

2. Key Laboratory of Marine Environment and Ecology, Ministry of Education, Ocean University of China, Qingdao 266100, China

3. Laboratory for Marine Ecology and Environmental Sciences, Qingdao National Laboratory for Marine Science and Technology, Qingdao 266071, China

4. Qingdao University of Science and Technology, Qingdao 266042, China

### ARTICLE INFO

#### Article history:

Received 30 July 2017

Revised 11 September 2018

Accepted 11 September 2018

Available online xxxx

#### Keywords:

CMAQ

Process analysis

PM<sub>2.5</sub>

Qingdao

### ABSTRACT

US EPA's Community Multiscale Air Quality modeling system (CMAQ) with Process Analysis tool was used to simulate and quantify the contribution of individual atmospheric processes to PM<sub>2.5</sub> concentration in Qingdao during three representative PM<sub>2.5</sub> pollution events in the winter of 2015 and 2016. Compared with the observed surface PM<sub>2.5</sub> concentrations, CMAQ could reasonably reproduce the temporal and spatial variations of PM<sub>2.5</sub> during these three events. Process analysis results show that primary emissions accounted for 72.7%–93.2% of the accumulation of surface PM<sub>2.5</sub> before and after the events. When the events occurred, primary emissions were still the major contributor to the increase of PM<sub>2.5</sub> in Qingdao, however the contribution percentage reduced significantly, which only account for 51.4%–71.8%. Net contribution from horizontal and vertical transport to the accumulation of PM<sub>2.5</sub> was also positive and its percentage increased when events occurred. Only 1.1%–4.6% of aerosol accumulation was due to PM processes and aqueous chemical processes before and after events. When the events occurred, contribution from PM processes and aqueous chemistry increased to 6.0%–11.8%. Loss of PM<sub>2.5</sub> was mainly through horizontal transport, vertical transport and dry deposition, no matter during or outside the events. Wet deposition would become the main removal pathway of PM<sub>2.5</sub>, when precipitation occurred.

© 2018 The Research Center for Eco-Environmental Sciences, Chinese Academy of Sciences.

Published by Elsevier B.V.

### Introduction

During the last several years, heavy regional air pollution events occurred repeatedly in China (Chan and Yao, 2008; Ye et al., 2011; Huang et al., 2012, 2014; Liu et al., 2013; Guo et al., 2014; Wang et al., 2014a, 2014c). PM<sub>2.5</sub> has become a hot topic across the country because of its key role in the pollution events and its harmful

effects on people's health. The occurrence of these severe PM<sub>2.5</sub> pollution events is still poorly understood, although a few hypotheses have been proposed to interpret the rapid formation and the accumulation of particulate pollutants (Wang et al., 2013; Zhang et al., 2015; Zheng et al. 2015).

Air quality models are important for the study of pollution events and air quality management because they assist in

\* Corresponding author.

E-mail address: [liuxh1983@ouc.edu.cn](mailto:liuxh1983@ouc.edu.cn). (X. Liu).

identifying source contributions to air quality problems and designing effective strategies to reduce air pollutants. US EPA's Community Multiscale Air Quality modeling system (CMAQ) has been widely used at regional or urban scales for the study of air pollution in China (Liu et al., 2010a, 2010b; Wang et al., 2015; Li et al., 2015; Cheng et al., 2014). For instance, Wang et al. (2015) used CMAQ to quantify the contributions of major source regions and sectors to  $PM_{2.5}$  concentrations in three most polluted cities in Hebei province. Li and Han (2015) applied CMAQ to quantifying the contribution of local emission and regional transport of pollutants to  $PM_{2.5}$  over Beijing-Tianjin-Hebei region. Similarly, Zhao et al., (2015) applied an innovative extended response surface modeling technique to identify the major sources contributing to  $PM_{2.5}$  and its inorganic components in the Yangtze River delta (YRD) region. Wang et al., (2014b) employed CMAQ model to simulate the impacts of aerosol-meteorology interactions on  $PM_{2.5}$  pollution during haze episode. Cheng et al., (2014) studied the impacts of biomass burning on haze pollution over the YRD region using WRF-CMAQ model. Che et al., (2011) assessed the impacts of five possible motor vehicle emission control measures on ambient air quality in Pearl River Delta (PRD) using CMAQ.

Several studies have also been performed to study the individual influential processes to the formation or accumulation of major pollutants in China using the process analysis tool in CMAQ (Liu et al., 2010b; Xing et al., 2011; Fan et al., 2015). Fan et al., (2015) used process analysis to explore aerosol characteristics and their formation mechanisms in the PRD region. Xing et al., (2011) applied CMAQ-PA tool to examine the influential processes and their sensitivity to the variation of emissions and meteorological conditions. Liu et al., (2010b) used the CMAQ model to study process analysis and sensitivity of ozone and particulate matter to precursor emissions during four seasons over China.

As illustrated above, the studies using CMAQ were mostly focus on the areas of Beijing-Tianjin-Hebei, YRD and

PRD. In addition, most of the studies pay attention to a single pollution event. In this article, we select Qingdao as the study region. Qingdao is an important national coastal city, it located the downwind area of the Northern China Plain (NCP), one of the most polluted regions in China (Sun et al., 2006; Chan and Yao 2008; Quan et al., 2011, 2014; Zhao et al., 2013). Hence, atmosphere composition in Qingdao is the combination of both anthropogenic pollutants from continent and natural pollutants from the marine atmosphere, which is distinguished from inland cities. High relative humidity caused by frequently occurred sea fog events in Qingdao is the favorable condition for aqueous phase reactions and lead to the production of secondary aerosols. Sea salt provides the probability of heterogeneous reactions of acid gases such as  $SO_2$ ,  $HNO_3$ ,  $N_2O_5$  which could influence the composition, concentration and even size distribution of  $PM_{2.5}$  (Gard et al., 1998; Athanasopoulou et al., 2008; Chen et al., 2016; Neumann et al., 2016). Although air quality in Qingdao is relatively better than that in Beijing-Tianjin-Hebei region,  $PM_{2.5}$  pollution events with the daily average value larger than  $100 \mu g/m^3$  still occurred frequently and the daily average values larger than  $300 \mu g/m^3$  were sometimes observed.

The objective of this study was that quantifying the contributions of individual atmospheric physical and chemical processes to  $PM_{2.5}$  accumulation and formation during three  $PM_{2.5}$  pollution events in Qingdao, which had different polluted levels.

## 1. Methodology

### 1.1. Model setup

CMAQ version 4.7.1 is applied over East Asia for the simulation during the winter of 2015 and 2016 (From December 11, 2015 to January 6, 2016; from December 12, 2016 to January 6, 2017). Fig. 1 shows the nested two domains, with the 36 km domain over East Asia, and the 12 km

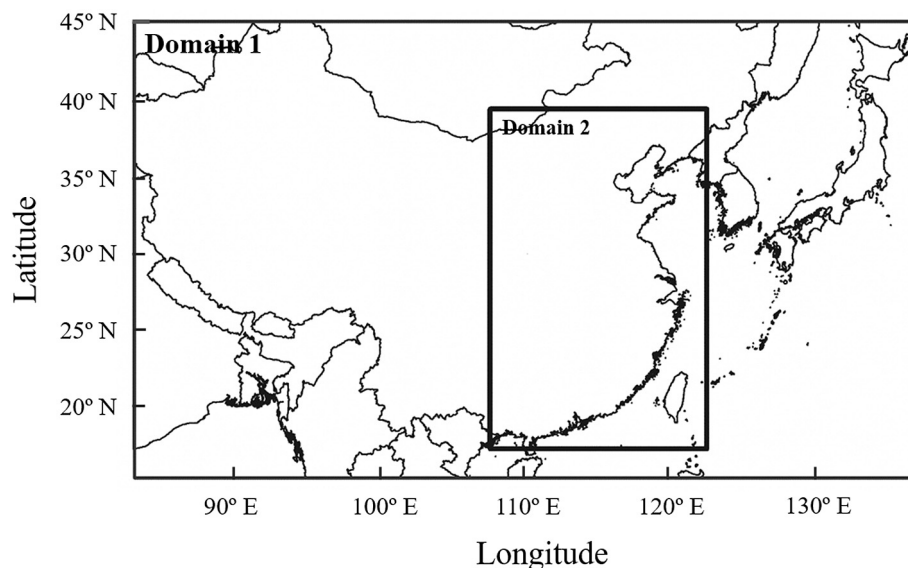


Fig. 1 – Two-nested modeling domains for CMAQ in this study.

domain over the eastern China. The vertical resolution includes 14 logarithmic structure layers from the surface to the troposphere, with the first model layer height of 36 m above the ground level. The gas-phase and aerosol modules were the CB05Cl mechanism (Sarwar and Luecken, 2008) and the AERO5 aerosol module. The meteorological fields are generated by The Weather Research & Forecasting Model (WRF) version 3.7. The National Centers for Environmental Prediction (NCEP) Final Analyses (FNL) data of  $1^\circ \times 1^\circ$  have been used to provide the initial (IC) and boundary conditions (BC) required by the WRF model. Terrain and surface type data are based on global data from the United States Geological Survey (USGS). The major physics options included Lin microphysics scheme (Lin et al., 1983), RRTM long-wave radiation scheme (Mlawer et al., 1997), Goddard short-wave scheme (Chou and Suarez, 1994), Monin-Obukhov surface-layer scheme (Obukhov, 1971), thermal diffusion land-surface scheme (Dudhia, 1996) and YSU land-surface scheme (Hong et al., 2006). The WRF hourly output files are processed with the Meteorology-Chemistry Interface Processor version 3.6. The Multi-resolution Emission Inventory for China (MEIC) for the base year 2012 was used in this study. Initial conditions and boundary conditions for Domain 1 were generated from a global chemistry model of GEOS-CHEM, and those for Domain 2 were extracted from Domain 1. A spin-up period of 7 days (December 4–10, 2015 and December 5–11, 2016) was used to eliminate the influence of initial conditions.

## 1.2. Observation data

Table 1 summarizes the observational data used for model evaluation in this study. The data of hourly  $PM_{2.5}$  concentration was obtained from the national air pollutant real-time observation data published by China National Environmental Monitoring Centre (<http://106.37.208.233:20035/>). Relevant meteorological data including wind direction, wind speed, ambient temperature and relative humidity were obtained from the Hong Kong University of Science and Technology atmospheric and environmental database (<http://envf.ust.hk/dataview/>). The synoptic weather charts were obtained from Korea Meteorological Administration (<http://web.kma.go.kr/chn/weather/images/analysis> chart.jsp).

## 1.3. Process analysis

Process analysis (PA) provided by the CMAQ model includes Integrated Process Rate (IPR) and Integrated Reaction Rate (IRR), and IPR can be used to identify and quantify the contribution of different physical and chemical processes to various chemical species such as surface  $PM_{2.5}$ . These

processes include emissions of primary species, horizontal transport, vertical transport, dry deposition, gas phase chemistry, cloud processes and PM processes. Horizontal transport is the sum of horizontal advection and diffusion, and vertical transport is the sum of vertical advection and diffusion. PM processes represent the net effect of aerosol thermodynamics, new particle formation, condensation of sulfuric acid and organic carbon on preexisting particles, and coagulation within and between Aitken and accumulation modes of PM. Cloud processes include the change of atmospheric photochemical rate resulted from the decrease of solar radiation caused by clouds, aqueous-phase chemistry, below and in-cloud mixing with chemical species, cloud scavenging, and wet deposition (Liu et al., 2010a, 2010b). In this paper, Integrated Process Rate was used to analyze the effect of various physical and chemical processes on  $PM_{2.5}$ .

## 1.4. Statistical analysis

The meteorological and air quality model performance were evaluated by statistical measures, including the correlation coefficient (R), normalized mean bias (NMB) and normalized mean error (NME). The NMB and NME were calculated by Eq. (1) and (2):

$$NMB = \frac{\sum_1^N (C_s - C_o)}{\sum_1^N C_o} \times 100\% \quad (1)$$

$$NME = \frac{\sum_1^N |C_s - C_o|}{\sum_1^N C_o} \times 100\% \quad (2)$$

where,  $C_s$  represents the simulated data,  $C_o$  represents the observational data and  $N$  is the number of data pairs.

## 1.5. Emission reduction scenarios

Air pollution events would be contributed by local or long range transport of air pollutants. In order to select the pollution events represented different types (local or long range transport), three emission reduction scenarios were designed to calculate contribution of  $PM_{2.5}$  from different regions (Fig. 2, Table 2). The contribution of one region to Qingdao was calculated by the equations below:

$$C_{i,con} = C_{Base} - C_i \quad (3)$$

$$P_{i,con} = \frac{C_{i,con}}{C_{Base}} \quad (4)$$

where,  $C_{i,con}$  and  $P_{i,con}$  are the concentration and percentage of each pollutant contribution from region  $i$ , respectively;  $C_{Base}$  and  $C_i$  are the simulated concentrations in base case and scenario case in region  $i$ .

**Table 1 – Observational data for model evaluation.**

Data set	Data	Variable	Frequency	Number	Sources
HKUST <sup>a</sup>	Meteorology	T2, RH2, WDS10, WDIR10	Hourly	1	<a href="http://envf.ust.hk/dataview/stnplot/current/">http://envf.ust.hk/dataview/stnplot/current/</a>
CNEMC <sup>b</sup>	$PM_{2.5}$	$PM_{2.5}$	Hourly	4	<a href="http://106.37.208.233:2003/">http://106.37.208.233:2003/</a>

<sup>a</sup> HKUST: meteorological data obtained from the Hong Kong University of Science and Technology's atmospheric and environmental database.  
<sup>b</sup> CNEMC: hourly  $PM_{2.5}$  concentrations obtained from the China National Environmental Monitoring Center.

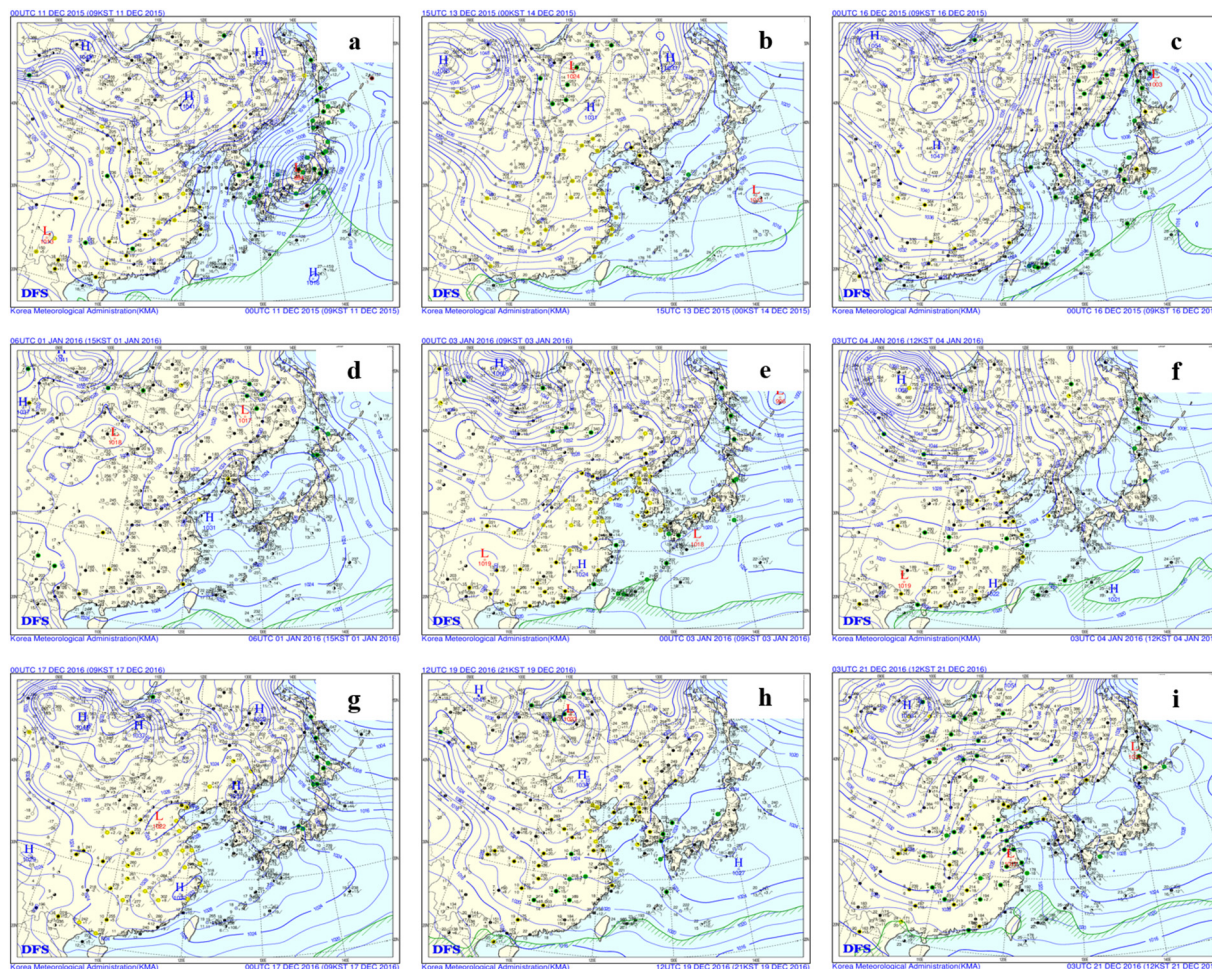


**Fig. 2 – Regions designed for emission reduction scenarios over domain 2 in this study. Region 1, include the southwest of Shandong, Anhui, Jiangsu and some of other regions; Region 2, include the northwest of Shandong province and most of Beijing-Tianjin- Hebei Region; Region 3, Qingdao.**

## 2. Model evaluation

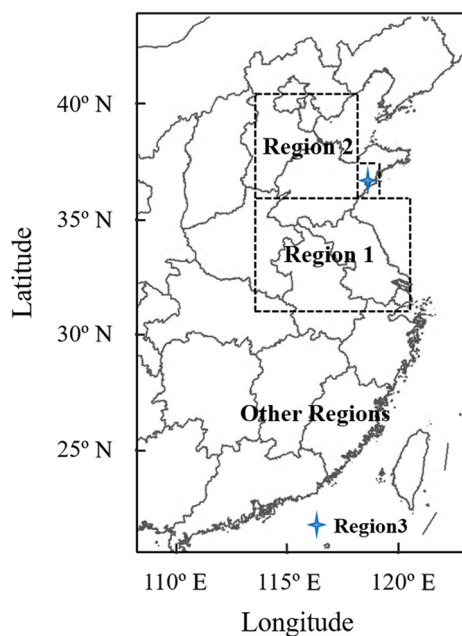
### 2.1. Evaluation of meteorological parameters

Fig. 3 shows the time variations of the observed and simulated temperature at 2 m (T2), relative humidity at 2 m (RH2), wind speed at 10 m (WSPD10) and wind direction at 10 m (WDIR10) in Qingdao during December 11, 2015–January 6, 2016 and December 12, 2016–January 6, 2017 at 12 km grid resolution. Table 3 summarizes the performance statistics of T2, RH2, WSPD10 and PM<sub>2.5</sub>. The temporal variations and magnitudes of T2 were well consistent with the observation, with the correlation coefficient of 0.9 and NMB of 39.4% during two winters (December 11, 2015–January 6, 2016 and December 12, 2016–January 6, 2017). WRF also gave out relatively good performance of RH2 except slightly overestimation during several hours (e.g. December 15–16, 2015), and the correlation coefficient and NMB of RH2 are 0.7 and 0.2%, respectively. Although the variation trend of the wind speed was well reproduced, the positive bias were sometimes occurred. From

the statistics results, the correlation coefficient between the simulated and observed wind speed is 0.8, while the NMB is 25.0%.

**Table 2 – Scenarios designed for the study of contributions from regional sources.**

Emission reduction scenarios		Purpose
Base case	Default emissions	
Source contribution of southwest area	Zeroing out Region 1 emissions	Evaluate the source contributions of the south of Shandong, Anhui and Jiangsu province, etc.
Source contribution of northwest area	Zeroing out Region 2 emissions	Evaluate the source contributions of the Beijing-Tianjin-Hebei region and the northwestern Shandong, etc.



**Fig. 3** – Time variations of observed and simulated meteorological variables in Qingdao: (a) hourly T2 (°C); (b) hourly RH2 (%); (c) hourly WSPD10 (m/sec); (d) hourly WDIR10 (degree).

The Yellow Sea is situated at the east and southeast directions of Qingdao, while at the northwest, west and southwest direction of Qingdao, it located strong industrial emissions of air pollutants. Therefore, wind direction is an important meteorological parameter that could influence the accuracy in predicting the contribution of the long range transport to the mass concentration of PM<sub>2.5</sub> in Qingdao. From Fig. 3, we can see that, obviously inconsistency between the observed and simulated of WDIR10 occurred during December 21–29, 2015, while during the rest time, WRF gave relatively better performance of WDIR10.

**Table 3** – Performance statistics of simulated meteorological conditions and PM<sub>2.5</sub> concentration in Qingdao.

	Mean Obs <sup>a</sup>	Mean Sim <sup>a</sup>	MB <sup>a</sup>	R <sup>a</sup>	NMB <sup>a</sup>	NME <sup>a</sup>
T2 <sup>b</sup>	1.8	2.5	0.7	0.9	39.4%	93.7%
RH2 <sup>b</sup>	70.7	70.8	0.1	0.7	0.2%	16.3%
WSPD10 <sup>b</sup>	3.0	3.5	0.5	0.8	25.0%	45.2%
PM <sub>2.5</sub> <sup>b</sup>	105.1	85.3	-19.8	0.7	-13.9%	45.2%
PM <sub>2.5</sub> <sup>c</sup>	85.8	82.3	-3.5	0.8	3.3%	42.6%

<sup>a</sup> Data pairs: the number of observed and simulated data pairs; Mean Obs: mean values of observational data; Mean Sim: mean values of simulation results; MB: mean bias; R: correlation coefficient; NMB: normalized mean bias.

<sup>b</sup> Definitions of these variables can be found in the footnotes of Table 1. The units of T2, RH2, WSPD10, PM<sub>2.5</sub> are °C, %, m/sec, µg/m<sup>3</sup> respectively. The T2, RH2, WSPD10 are evaluated using hourly data.

<sup>c</sup> The performance statistics during December 11–18, December 27–29 in 2015, January 1–6, December 12–30 in 2016 and January 1–6 in 2017.

## 2.2. Evaluation of surface concentrations of PM<sub>2.5</sub> and its components

Fig. 4 shows the observed and simulated temporal variations of surface concentrations of PM<sub>2.5</sub> in Qingdao during the winter of 2015 and 2016. The performance statistics of meteorological parameters and PM<sub>2.5</sub> are summarized in Table 3. During December 11, 2015–January 6, 2016 and December 12, 2016–January 6, 2017, several PM<sub>2.5</sub> pollution events occurred in Qingdao. CMAQ could captured the variation trends of PM<sub>2.5</sub> during most of these events (Fig. 4). In terms of the magnitude, simulated concentrations of PM<sub>2.5</sub> and its components are well predicted during December 11–18, 27–29, 2015, January 1–6, 2016 and December 12, 2016 January 6, 2017, but obviously underestimated during December 19–26 and 30–31, 2015. The correlation coefficient R of PM<sub>2.5</sub> was 0.7 during the simulated period. However, the R values increased up to 0.8, when PM<sub>2.5</sub> values during December 19–26 and 30–31, 2015 were not included.

## 3. Results and discussion

According to the above analysis, several PM<sub>2.5</sub> pollution events occurred in Qingdao during the winter of 2015 and 2016, CMAQ showed good performance during most events. According to the results of emission reduction scenarios analysis (Fig. 5), we selected three representative events for analysis. The first event started from 21:00 on December 13 and ended at 3:00 on December 15, 2015, the second event occurred during 0:00 on January 2 to 8:00 on January 4, 2016, and the third event occurred during 00:00 December 19 to 9:00 December 21. Pollutants from outside of Qingdao were the main contributor to PM<sub>2.5</sub> in Qingdao during Event 1, Event 2 and the latter part of Event 3. While during the first part of Event 3, primary emissions was the dominate contributor to PM<sub>2.5</sub> in Qingdao.

### 3.1. Characteristics of three PM<sub>2.5</sub> events

#### 3.1.1. Weather circulation conditions during three events

Fig. S1 in supplement gives out the synoptic weather charts at surface level during three PM<sub>2.5</sub> pollution events. At 8:00 on December 11, 2015 (before Event 1), Qingdao was located at the bottom of high pressure, the isobars were relatively intensive. The northwest wind was blowing at this time in Qingdao and the wind speed was 7 m/sec. At 23:00 on December 13, 2015 (during Event 1), the isobars was sparse and the wind speed decreased to less than 3 m/sec. Poor atmospheric diffusion conditions was conducive to the accumulation of pollutants. Also, the surface relative humidity increased in Qingdao, providing a favorable environment for aqueous chemistry reactions and pollutants moisture absorption growing. At 8:00 on December 16, 2015 (after Event 1), due to the influence of weak cold front, the isobars in Qingdao significantly become intense, and the wind speed increased to 7 m/sec, which promoted the diffusion of pollutants.

At 8:00 on January 1, 2016 (before Event 2), Qingdao was located at the rear of the high pressure system and had a

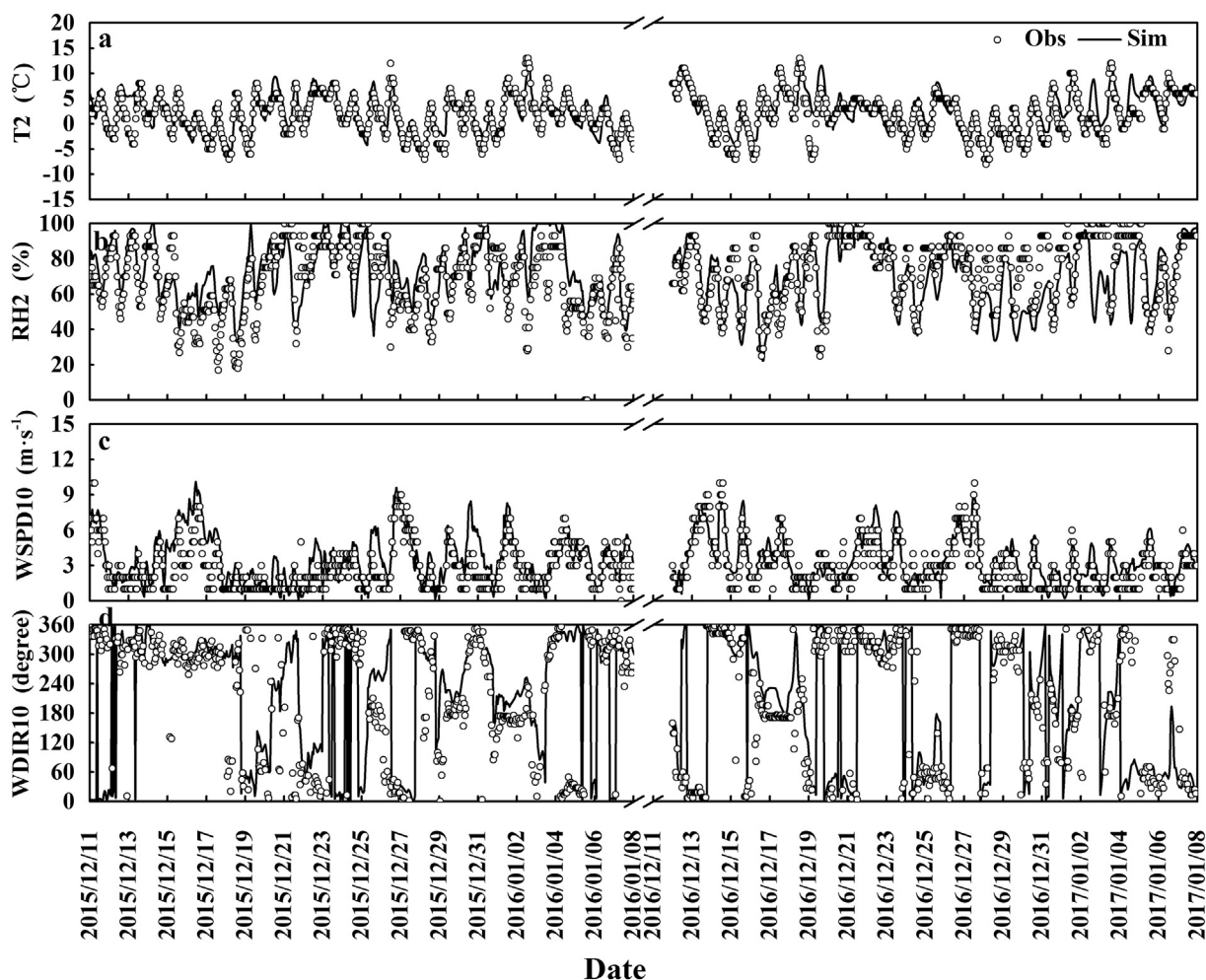


Fig. 4 – Time variations of observed and simulated hourly  $PM_{2.5}$  concentrations in Qingdao (Unit:  $\mu g/m^3$ ).

warm southwesterly airflow at surface level, which was conducive to the transmission of upwind pollutants. At 8:00 on January 3, 2016 (during Event 2), Qingdao area was located at the uniform pressure field at the bottom of cold high pressure, with the wind speed of 2 m/sec, and the atmosphere stratification was stable which lead to poor atmospheric diffusion conditions and continuous accumulation of pollutants. Relative humidity at this time was higher than 90%, it provided a suitable environment for the production of secondary aerosol. At 11:00 on January 4, 2016 (after Event 2), the high pressure system in the west of Baikal was strengthened and pushed southward. Affected by the cold air, the pressure gradient in the Qingdao area increased, the wind speed increased, and pollutants dissipated.

At 8:00 on December 17, 2016 (before Event 3), Qingdao was located between the high and low pressure system, and had a southerly airflow at surface level. When the pollution occurred, Qingdao area was controlled by uniform pressure field, the pressure gradient was small, and the diffusion conditions were poor. However, at 20:00 on December 19, 2016 (the latter part of Event 3), pollutants may transported into Qingdao area under the northerly airflow with the Mongolian high-pressure southward. At 11:00 on December 21, 2016

(after Event 3), the center position of depression which located in the YRD moves northward and the strength of depression increased. Influenced by the southwest warm moist current in front of the trough, precipitation occurred in Qingdao.

### 3.1.2. Characteristics of $PM_{2.5}$ concentrations in Qingdao during three events

Fig. 4 shows the temporal variations of observed and simulated hourly  $PM_{2.5}$  concentrations in Qingdao. During the first event,  $PM_{2.5}$  in Qingdao continuously and slowly increased from  $68 \mu g/m^3$  at 20:00 on December 13, 2015 to the peak concentration of  $\sim 150 \mu g/m^3$  at 23:00 on December 14, 2015, then it gradually decreased to  $80 \mu g/m^3$  at 3:00 on December 15. During the second event,  $PM_{2.5}$  in Qingdao abruptly increased from  $103 \mu g/m^3$  at 0:00 on January 2 to  $309 \mu g/m^3$  at 19:00 on January 3. Since then,  $PM_{2.5}$  started to decrease, and reached to about  $80 \mu g/m^3$  at 8:00 on January 4, 2016. During the third event, surface  $PM_{2.5}$  in Qingdao continuously and slowly increased from  $35 \mu g/m^3$  at 10:00 on December 16 to the concentration of  $\sim 200 \mu g/m^3$  at December 19, 2016 and then fluctuated until 9:00 on December 21, the concentration of  $PM_{2.5}$  dropped rapidly to  $59 \mu g/m^3$  at 10:00 on December 21, 2016.

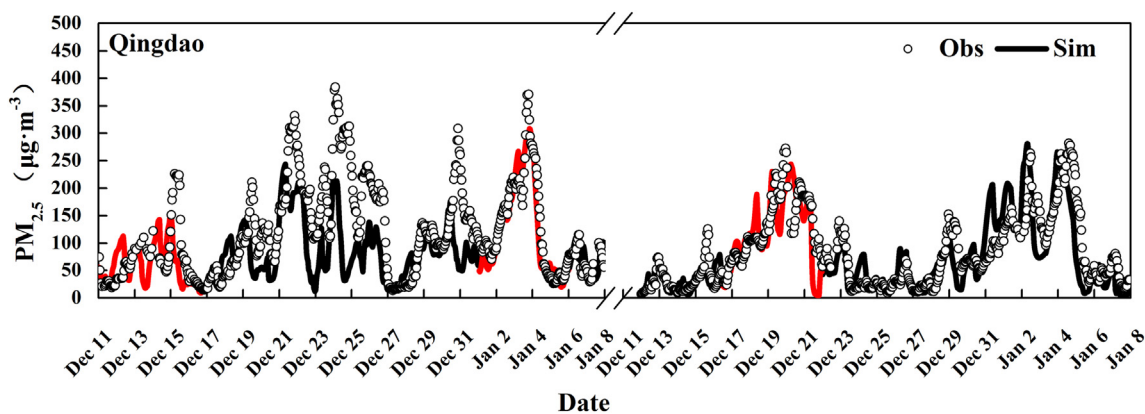


**Fig. 5** – Percentage contribution to Qingdao  $PM_{2.5}$  from different regions during three  $PM_{2.5}$  events. (a) the first  $PM_{2.5}$  pollution event, (b) the second  $PM_{2.5}$  pollution event, (c) the third  $PM_{2.5}$  pollution event. (Unit: %).

### 3.1.3. Regional characteristics of $PM_{2.5}$ concentrations during three $PM_{2.5}$ events

Figs. 6–8 show the spatial distributions of daily averaged  $PM_{2.5}$  concentrations over East China during December 11–16, 2015, January 1–5 and December 16–21, 2016. The first regional  $PM_{2.5}$  event initially occurred over Beijing and Tianjin area on December 11, with the highest daily averaged  $PM_{2.5}$  concentration  $\sim 175$ – $200 \mu\text{g}/\text{m}^3$ . At the same time,  $PM_{2.5}$  in Qingdao was as low as  $\sim 25$ – $50 \mu\text{g}/\text{m}^3$ . On December 12–13, the area with high  $PM_{2.5}$  expanded rapidly.  $PM_{2.5}$  concentration over Beijing-Tianjin-Hebei Region, Shanxi and Henan province increased to  $>150 \mu\text{g}/\text{m}^3$ . Although  $PM_{2.5}$  mass concentrations over Qingdao was slightly increased on December 12–13 ( $50$ – $75 \mu\text{g}/\text{m}^3$ ), it was still much lower than that over Beijing-Tianjin-Hebei Region. On December 14,  $PM_{2.5}$  concentrations over Beijing-Tianjin-Hebei Region and Henan, Anhui, Jiangsu area were in the range of  $200$ – $250 \mu\text{g}/\text{m}^3$ . Daily averaged  $PM_{2.5}$  concentration in Qingdao rapidly increased from  $75 \mu\text{g}/\text{m}^3$  to nearly  $120 \mu\text{g}/\text{m}^3$ . On December 15, the area with relatively  $PM_{2.5}$  concentration moved to YRD area, while  $PM_{2.5}$  concentration in Qingdao decreased to  $15 \mu\text{g}/\text{m}^3$ . On December 16, the concentration of  $PM_{2.5}$  over entire Domain 2 decreased to  $<50 \mu\text{g}/\text{m}^3$ . (See Fig. 6.)

The second regional  $PM_{2.5}$  event initially happened over Tianjin-Beijing, Tangshan-Baoding-Shijiazhuang area (on January 1, 2016), showing zonal distribution, with the highest daily averaged  $PM_{2.5}$  concentration was  $\sim 200$ – $350 \mu\text{g}/\text{m}^3$ .  $PM_{2.5}$  over west of Shandong and Jiangsu, south of Hebei and east of Henan province were in the range of  $\sim 100$ – $150 \mu\text{g}/\text{m}^3$  and it was lower than  $100 \mu\text{g}/\text{m}^3$  in Qingdao. Similarly to the first event, area with significantly high concentration of  $PM_{2.5}$  quickly expanded on the second day.  $PM_{2.5}$  concentration over Henan and west of Shandong province increased from  $<150$  to  $\sim 200 \mu\text{g}/\text{m}^3$ .  $PM_{2.5}$  concentration in Qingdao increased from  $<100$  to  $\sim 150 \mu\text{g}/\text{m}^3$  rapidly. On January 3, the border of Shanxi and Henan province, south of Shandong, west of Henan, north of Anhui and Jiangsu province showed  $PM_{2.5}$  concentrations higher than  $250 \mu\text{g}/\text{m}^3$ . Daily averaged  $PM_{2.5}$  concentration in Qingdao reached its maximum of  $\sim 300 \mu\text{g}/\text{m}^3$ . On January 4,  $PM_{2.5}$  mass concentrations over Anhui,

Jiangsu area were in the range of  $250$ – $350 \mu\text{g}/\text{m}^3$ , while in Qingdao,  $PM_{2.5}$  significantly decreased from  $275$  to  $100 \mu\text{g}/\text{m}^3$ . On January 5, the concentration of  $PM_{2.5}$  over whole Domain 2 decreased to  $<50 \mu\text{g}/\text{m}^3$ . (See Fig. 7.)

Similarly, the third regional  $PM_{2.5}$  event initially started over Beijing-Tianjin-Hebei area on December 16, 2016, with the daily averaged  $PM_{2.5}$  concentration was  $\sim 150$ – $200 \mu\text{g}/\text{m}^3$  (Fig. 8a). At the same time,  $PM_{2.5}$  concentration in Qingdao was lower than  $80 \mu\text{g}/\text{m}^3$ . On December 18,  $PM_{2.5}$  concentrations over Beijing-Tianjin-Hebei area increased to higher than  $200 \mu\text{g}/\text{m}^3$  and pollution zone ( $PM_{2.5} > 200 \mu\text{g}/\text{m}^3$ ) extended to the Northwest of Shandong province.  $PM_{2.5}$  concentration in Qingdao increased from  $<80$  to  $\sim 150 \mu\text{g}/\text{m}^3$ . On December 19 and 20,  $PM_{2.5}$  concentrations over Beijing-Tianjin-Hebei area increased to higher than  $300 \mu\text{g}/\text{m}^3$ . The zone with  $PM_{2.5} > 300 \mu\text{g}/\text{m}^3$  spread to Henan, Southwestern of Shandong province, etc. Simultaneously, daily averaged  $PM_{2.5}$  concentration in Qingdao reached its maximum of  $\sim 250 \mu\text{g}/\text{m}^3$ . On December 22, due to precipitation,  $PM_{2.5}$  in Qingdao dropped to  $\sim 50 \mu\text{g}/\text{m}^3$ . (See Fig. 8.)

Temporal variation of  $PM_{2.5}$  in Qingdao and the spatial distribution of  $PM_{2.5}$  over East China indicated that the intensity of events, the moving routes, the ages of the events and the areas covered by the events were different. Such differences suggested that the formation mechanisms of three  $PM_{2.5}$  events in Qingdao may be different, which need to be further discussed.

### 3.2. Analysis of integrated process rates (IPR) on surface $PM_{2.5}$

Fig. 9 shows the hourly contributions of individual atmospheric physical and chemical processes to variations of surface  $PM_{2.5}$  mass concentrations during December 11–16, 2015 (a), January 1–5, 2016 (b) and December 16–22, 2016 (c).

Before the first event (0:00 on December 11, 2015–20:00 on December 13, 2015), primary emissions acted as the dominate contributor to the surface  $PM_{2.5}$  in Qingdao, accounting for  $\sim 88.1\%$  of accumulation of  $PM_{2.5}$  mass concentrations. PM processes might either serve as a sink or a source for  $PM_{2.5}$  before the first event. Its contribution to

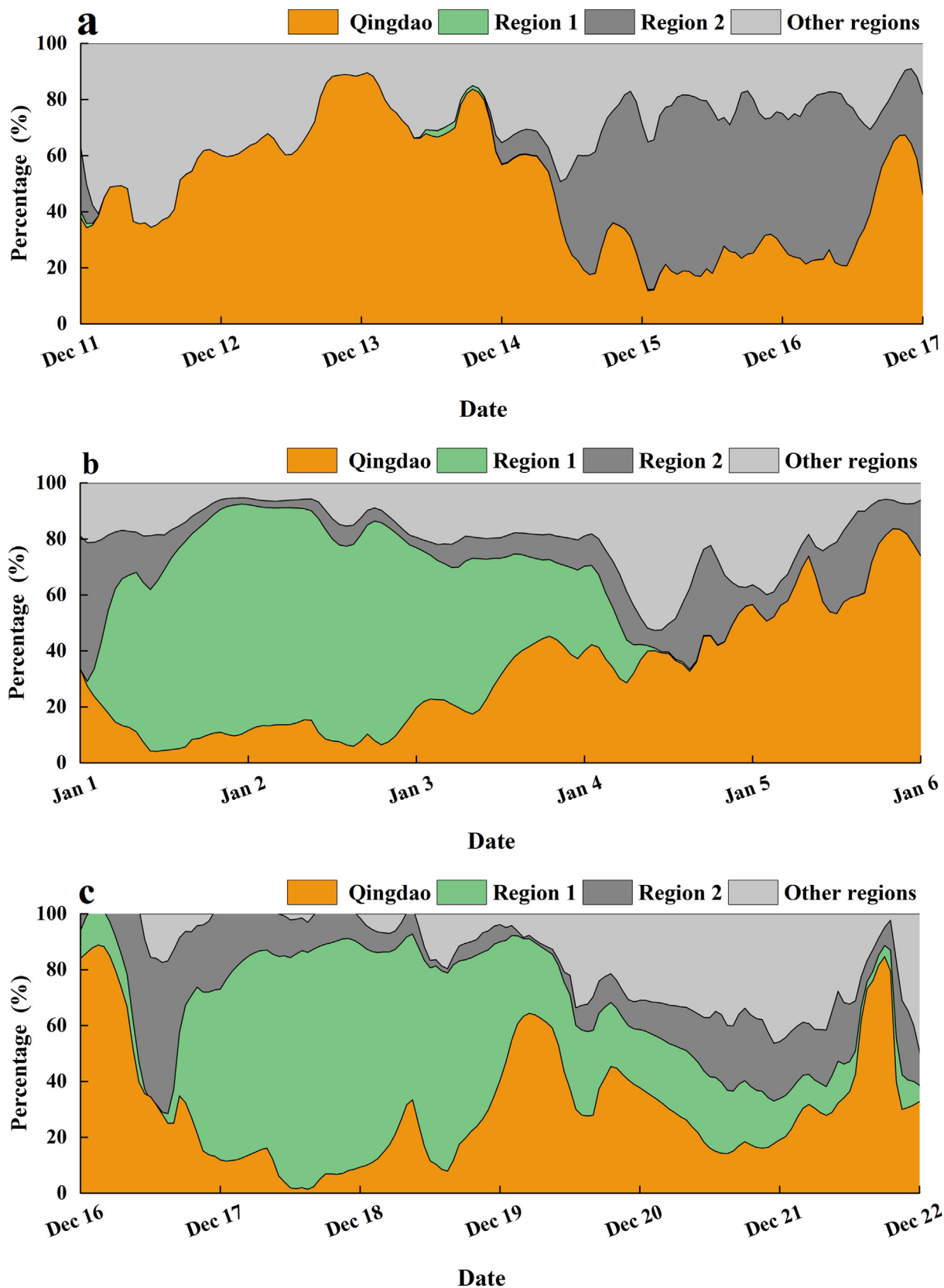
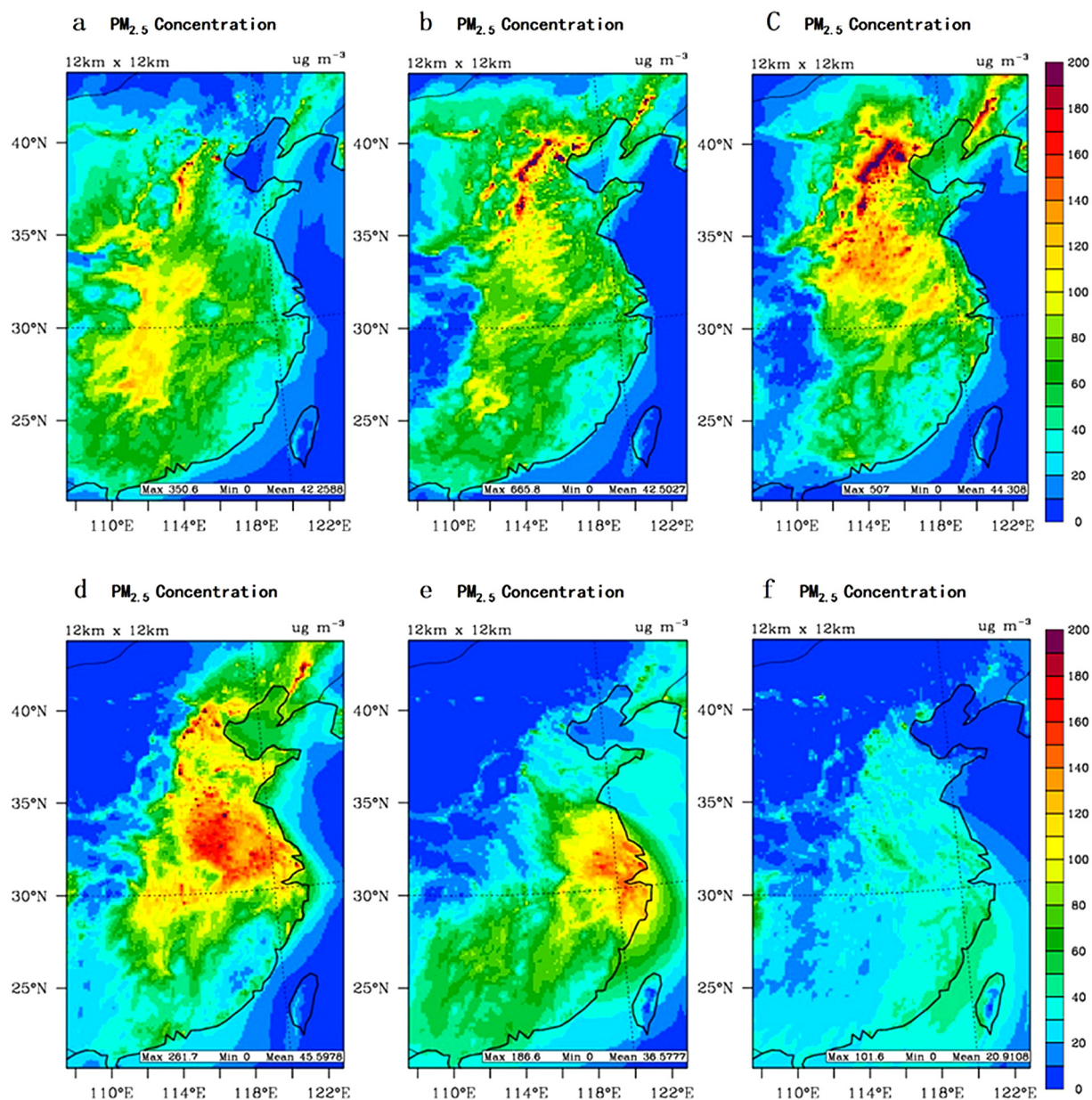


Fig. 6 – Spatial distributions of simulated daily mean concentrations of  $PM_{2.5}$  over eastern China during December 11–16, 2015 (a, b, c, d, e, f are CMAQ simulated  $PM_{2.5}$  on December 11–16, 2015, respectively) (Unit:  $\mu g/m^3$ ).



**Fig. 7 – Spatial distributions of simulated daily mean concentrations of  $PM_{2.5}$  over eastern China during January 1–6, 2016 (a, b, c, d, e are CMAQ simulated  $PM_{2.5}$  on January 1–5, 2016, respectively) (Unit:  $\mu\text{g}/\text{m}^3$ ).**

accumulation of  $PM_{2.5}$  was smaller, accounting for ~4.4%, while its negative effect to  $PM_{2.5}$  during the first event was ~1.9%. Horizontal and vertical transport mainly acted as removal pathways of  $PM_{2.5}$ , accounting for ~14.8% and ~76.4%, respectively. As a sink for  $PM_{2.5}$ , dry deposition amount depends on particulate concentration and the rate of dry deposition (Fan et al., 2015). The PA results after the first event (4:00 on December 15–23:00 on December 16) was similar to that before the first event. Emissions were still the main contributors to accumulation of  $PM_{2.5}$  mass concentrations, accounting for ~92.5%. Vertical transport and horizontal transport were still major contributors for the removal of  $PM_{2.5}$ , accounting for ~50.2% and ~41.1% respectively.

When the first event occurred (21:00 on December 13, 2015–3:00 on December 15, 2015), contributions of individual atmospheric processes to  $PM_{2.5}$  in Qingdao were different from that before or after the event. Although primary emissions (71.8%) still accounted for a large proportion to accumulation of  $PM_{2.5}$ , vertical transport gradually became the significant contributor to the accumulation of surface  $PM_{2.5}$ , accounting for 19.3%. The positive contribution from vertical transport would be related to the significantly lower PBL height during this period than that before and after the event (Fig. 10). Total contribution rate of horizontal and vertical transport was ~19.7%, which was significantly higher than before and after the event. Secondary formation of aerosol accounted for ~7.3% of accumulation of  $PM_{2.5}$  through PM processes and ~1.2%

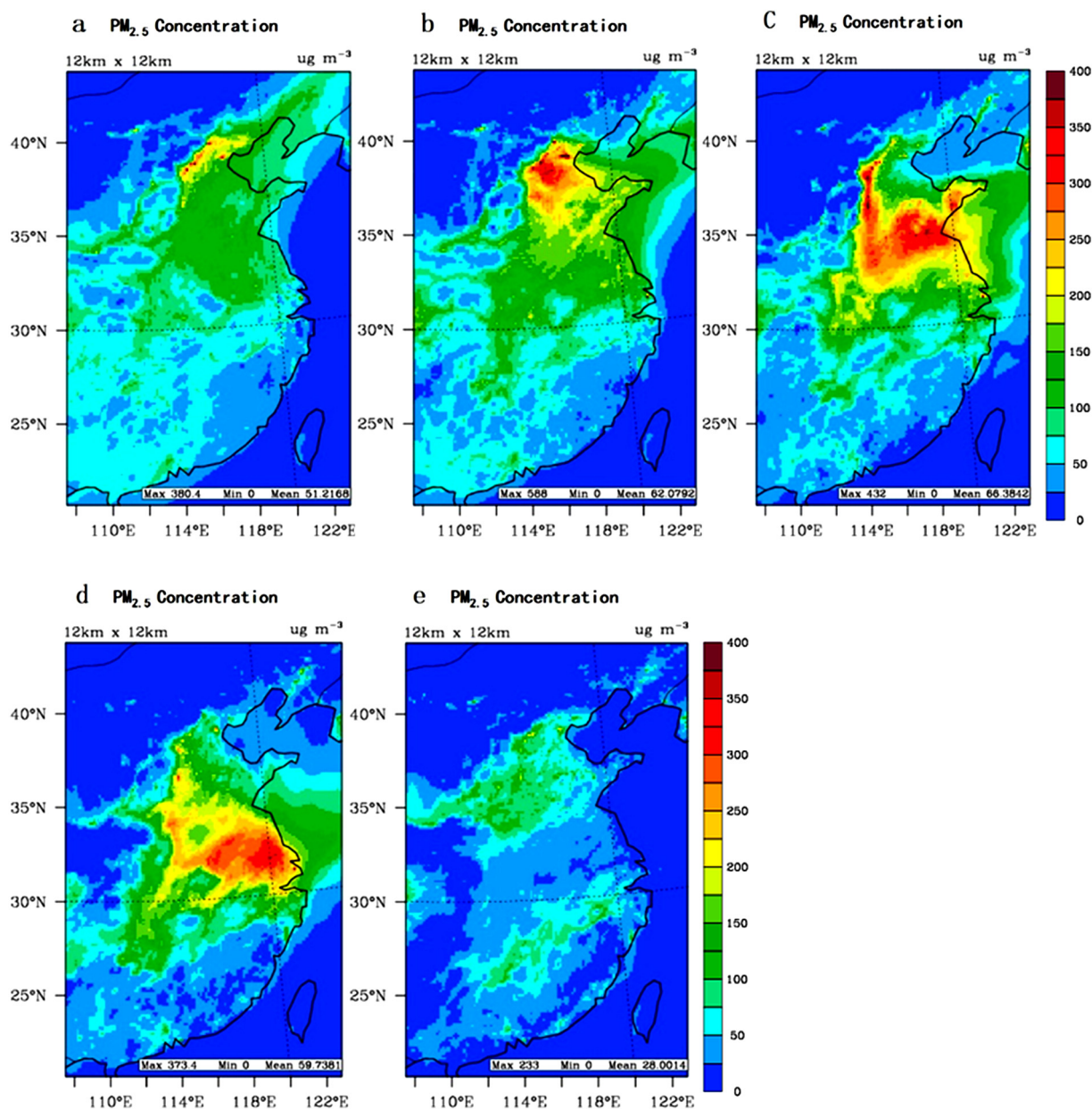


**Fig. 8** – Spatial distributions of simulated daily mean concentrations of  $PM_{2.5}$  over eastern China during December 16–22, 2016 (a, b, c, d, e are CMAQ simulated  $PM_{2.5}$  on December 16 17 18 19 20 22, 2016, respectively) (Unit:  $\mu g/m^3$ ).

through aqueous-phase oxidation of  $SO_2$ . Particularly, the contribution of PM processes mainly occurred during the rise period of the  $PM_{2.5}$  concentration. Its maximum contribution rate occurred at 15:00 on December 14, which accounted for 12.3% (Fig. 9). Horizontal transport and vertical transport were the major negative contributor to surface  $PM_{2.5}$  during the first event, accounting for ~72.7% and ~16.6% of total depletion of  $PM_{2.5}$  mass concentrations. At the same time, dry deposition also played a negative role in  $PM_{2.5}$  mass concentrations which contributed approximately ~10.5%.

Event 2: before and after the second event (0:00–23:00 on January 1, 2016 and 9:00 on January 4–23:00 on January 5, 2016), emissions of primary pollutants from local or regional

sources were also the dominate positive contributor to accumulation of surface  $PM_{2.5}$  in Qingdao, the contribution rate before and after the event was 92.0% and 93.2%, respectively, which was similar to the period before and after the first event. The contribution rate of PM processes was 4.3% and 4.0%, respectively. Total contribution rate of horizontal and vertical transport before and after the event was 3.6% and 2.8%, respectively. However, the contribution of the aqueous phase process was almost negligible. Vertical transport, horizontal transport and dry deposition all reduced  $PM_{2.5}$  mass concentrations before and after the second event. Among them, horizontal transport was the dominate sink of  $PM_{2.5}$  before the event, accounting for average 57.6% of total

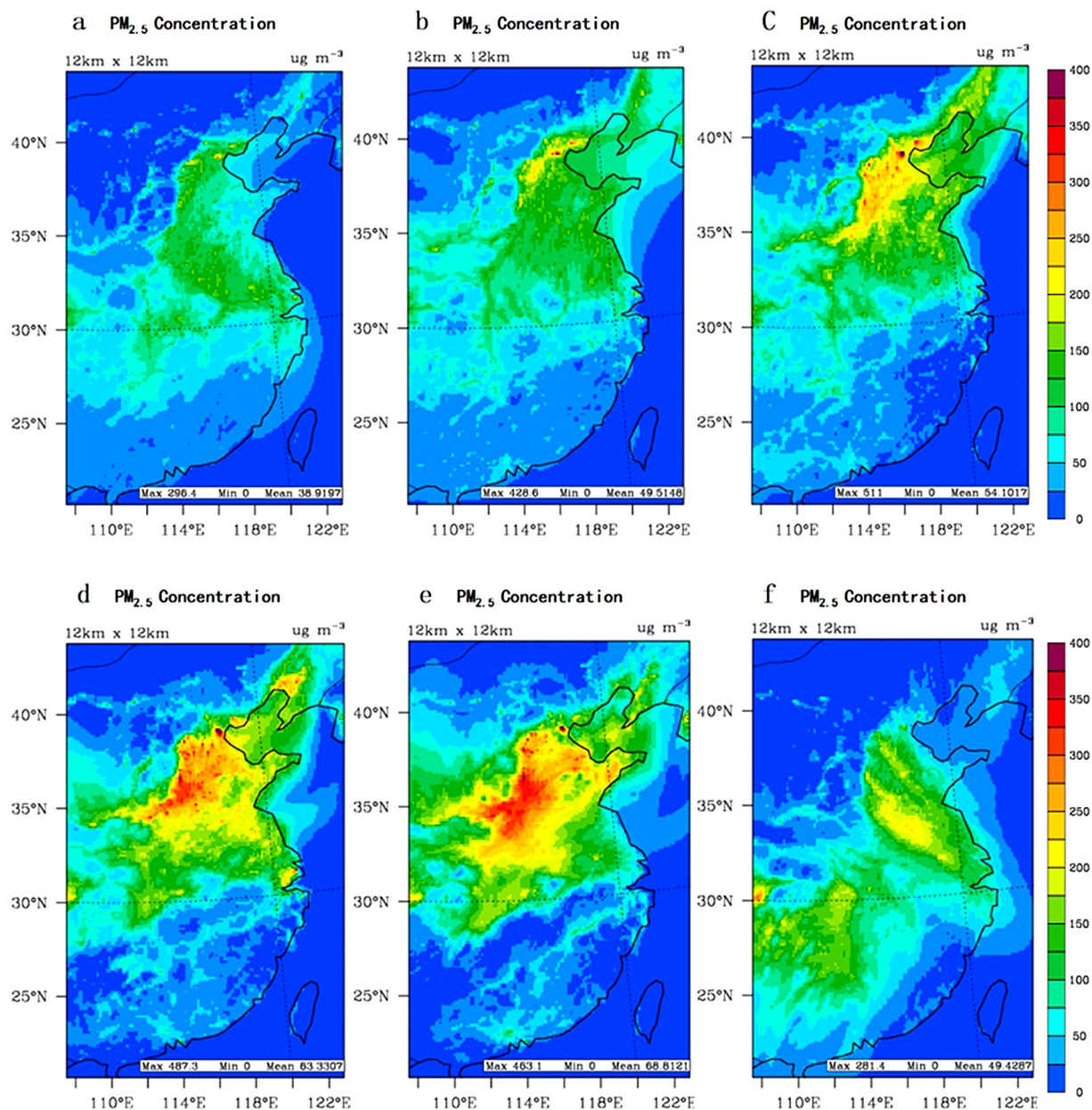


**Fig. 9 – Time variations of  $PM_{2.5}$  contributions from various physical and chemical processes in the near-surface layer above the Qingdao station during (a) the first pollution event, (b) the second pollution event, (c) the third pollution event (Unit:  $\mu\text{g}/\text{m}^3/\text{hr}$ ).**

depletion. Vertical transport was the dominate sink of  $PM_{2.5}$  after the event (73.5% of total  $PM_{2.5}$  depletion).

During the second event in Qingdao (0:00 on January 2, 2016–8:00 on January 4, 2016), emissions were the major source of  $PM_{2.5}$  consistently, however its contribution rate for accumulation of  $PM_{2.5}$  dropped sharply to 51.4%. Positive contribution of horizontal and vertical transport increased significantly, accounting for  $\sim 17.8\%$  and  $\sim 24.5\%$ , respectively. Secondary aerosol formation through PM processes declined slightly, however aqueous phase chemistry was obviously more effective, which accounted for  $\sim 3.8\%$  of total accumulation of  $PM_{2.5}$  mass concentrations. Horizontal and vertical transport were also the main processes for  $PM_{2.5}$  removal,

which accounting for 54.4% and 32.8% of the loss of  $PM_{2.5}$ . Also,  $PM_{2.5}$  was also reduced by dry deposition (6.8%) and PM processes (6.1%).

Event 3: before and after the third event (10:00 on December 16–23:00 on December 18 and 10:00 on December 21–23:00 on December 21), positive contribution from primary emissions to surface  $PM_{2.5}$  in Qingdao accounted for  $\sim 73\%$ . Horizontal transport was an important source for  $PM_{2.5}$  beside primary emissions, which accounted for 20.0%–26.3%. But the positive contribution of vertical transport was low ( $\sim 2.5\%$ ). Both vertical and horizontal transport also acted main sinks for  $PM_{2.5}$  in Qingdao before Event 3, accounting for 29.3% and 61.1%, respectively. After this event,  $PM_{2.5}$  was obviously

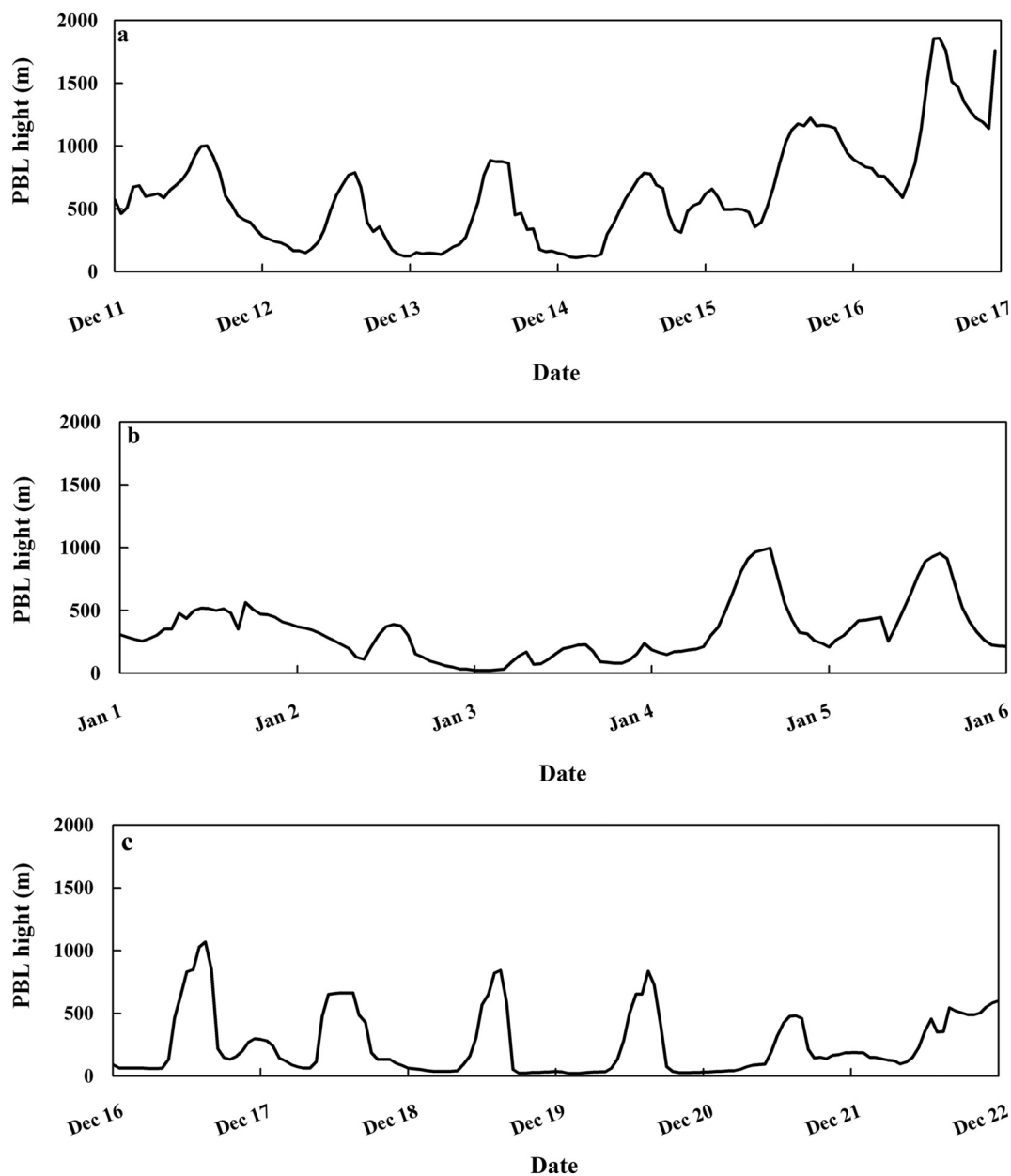


**Fig. 10 – Time variations of simulated PBL height (Unit: m). (a) the first  $PM_{2.5}$  pollution event, (b) the second  $PM_{2.5}$  pollution event, (c) the third  $PM_{2.5}$  pollution event.**

washed out via wet deposition and vertical transport, which accounted for 35.4% and 44.7%, respectively.

During the first part of Event 3 (00:00 on Dec 19 9:00 on Dec 19), contribution from primary emissions to the accumulation of  $PM_{2.5}$  reduced to ~57.2%. Contribution of horizontal transport also reduced, however the total contribution of horizontal and vertical transport increased (31.0%). Increased positive contribution was also from PM process (~11.8%). During the latter part of Event 3 (10:00 on Dec 19 9:00 on Dec 21), accumulation of  $PM_{2.5}$  was due to the combination of primary emissions (~56.3%) and horizontal transport (~35.2%). The contribution of secondary aerosols formation through PM process and aqueous phase chemistry declined to 6.0%. Removal of  $PM_{2.5}$  during this event was mainly due to horizontal and vertical transport and dry deposition.

Compared with the results of three events, we could draw that primary emissions were the dominate contributor to the surface  $PM_{2.5}$  in all events. Before or after the events, the contribution of the primary emissions was over 70%. When events occurred, the contribution of primary emissions reduced significantly, horizontal transport and vertical transport increased. Simultaneously, the contribution of PM processes and aqueous chemical processes which related to secondary formation of aerosols also increased, especially during the rapid rise of  $PM_{2.5}$ . During the events or before and after the events, the removal of  $PM_{2.5}$  was mainly through horizontal transport, vertical transport. The contribution rate of dry deposition was almost unchanged, which was 5.9%–11.8%. The only exception was when precipitation occurred, wet deposition become the main process of  $PM_{2.5}$  removal.

#### 4. Conclusions

The PA tool embedded in CMAQ is applied to quantify the contributions of individual atmospheric processes to the formation of PM<sub>2.5</sub> during three representative pollution events and the model performances are satisfied during these three events.

Contributions from individual atmospheric processes to accumulation or loss of PM<sub>2.5</sub> were different among three events and also different during different stages of each event. Primary emissions were the dominate contributor to accumulation of surface PM<sub>2.5</sub> in all periods. Before or after the events, primary emissions to accumulation of surface PM<sub>2.5</sub> accounted for 72.7%–93.2%. When the pollution occurred, primary emissions were still the major contributor, but the contribution rate reduced significantly (51.4%–71.8%). Different from primary emissions, the contribution rate of horizontal transport and vertical transport to accumulation of PM<sub>2.5</sub> increased from 2.8%–26.3% to 19.7%–42.2% when events occurred. Simultaneously, the production of secondary aerosols through PM processes and aqueous chemical processes increased from 1.1%–4.6% to 6.0%–11.8%, especially during the rapid rise period of PM<sub>2.5</sub>.

For removal pathways of PM<sub>2.5</sub> was mainly through horizontal transport and vertical transport. The contribution rate of dry deposition to removal of PM<sub>2.5</sub> was in the range of 5.9% to 11.8%. When precipitation occurred, wet deposition become the main removal pathway of PM<sub>2.5</sub> (35.4%).

Supplementary data to this article can be found online at <https://doi.org/10.1016/j.jes.2018.09.007>.

#### Acknowledgments

This research was supported by the National Natural Science Foundation of China (Nos. 41430646, 41305087); the Shandong Provincial Natural Science Foundation, China (No. ZR2013DQ022); the National Key Basic Research Program of China (No. 2014CB953701); the Qingdao science and technology project (14-8-3-10-NSH). Thanks are given to Prof. Qiang Zhang from Tsinghua University who kindly provided us the MEIC emission inventory over East Asia for the study. And we thank Prof. Shan hong Gao from Ocean University of China for us providing meteorological data.

The following are the supplementary data related to this article.

#### REFERENCES

Athanasopoulou, E., Tombrou, M., Pandis, S.N., Russell, A.G., 2008. The role of sea-salt emissions and heterogeneous chemistry in the air quality of polluted coastal areas. *Atmos. Chem. and Phys.* 8 (1), 3807–3841.

Chan, C.K., Yao, X.H., 2008. Air pollution in mega cities in China. *Atmos. Environ.* 42 (1), 1–42.

Che, W.W., Zheng, J.Y., Wang, S.S., Zhong, L.J., Lau, A., 2011. Assessment of motor vehicle emission control policies using Model-3/CMAQ model for the Pearl River Delta region, China. *Atmos. Environ.* 45 (9), 1740–1751.

Chen, Y., Cheng, Y.F., Ma, N., Wolke, R., Nordmann, S., Schuttauf, S., et al., 2016. Sea salt emission, transport and influence on size-segregated nitrate simulation: a case study in northwestern Europe by WRF-Chem. *Atmos. Chem. Phys.* 16 (18), 12081–12097.

Cheng, Z., Wang, S., Fu, X., Watson, J.G., Jiang, J., Fu, Q., et al., 2014. Impact of biomass burning on haze pollution in the Yangtze River delta, China: a case study in summer 2011. *Atmos. Chem. Phys.* 14 (9), 4573–4585.

Chou, M.D., Suarez, M.J., 1994. An efficient thermal infrared radiation parameterization for use in general circulation models. *NASA Tech. Memo.* 104606 (3), 85.

Dudhia, J., 1996. A multi-layer soil temperature model for MM5. The Sixth PSU/NCAR mesoscale model users' workshop. Colo, USA. Jul 22–24.

Fan, Q., Lan, J., Liu, Y., Wang, X.M., Chan, P., Hong, Y.Y., et al., 2015. Process analysis of regional aerosol pollution during spring in the Pearl River Delta region, China. *Atmos. Environ.* 122, 829–838.

Gard, E.E., Kleeman, M.J., Gross, D.S., Hughes, L.S., Allen, J.O., Morrical, B.D., et al., 1998. Direct Observation of Heterogeneous Chemistry in the Atmosphere. *Science* 279 (5354), 1184–1187.

Guo, S., Hu, M., Zamora, M.L., Peng, J.F., Shang, D.J., Zheng, J., et al., 2014. Elucidating severe urban haze formation in China. *Proc. Natl. Acad. Sci.* 111 (49), 17373–17378.

Hong, S.Y., Noh, Y., Dudhia, J., 2006. A new vertical diffusion package with an explicit treatment of entrainment processes. *Mon. Weather Rev.* 134 (9), 2318–2341.

Huang, K., Zhuang, G., Lin, Y., Wang, Q., Fu, J.S., Zhang, R., et al., 2012. Impact of anthropogenic emission on air quality over a megacity—revealed from an intensive atmospheric campaign during the Chinese Spring Festival. *Atmos. Chem. Phys.* 12 (23), 11631–11645.

Huang, R.J., Zhang, Y.L., Bozzetti, C., Ho, K.F., Cao, J.J., Han, Y.M., et al., 2014. High secondary aerosol contribution to particulate pollution during haze events in China. *Nature* 514 (7521), 218–222.

Li, J.W., Han, Z.W., 2015. A modeling study of severe winter haze events in Beijing and its neighboring regions. *Atmos. Res* 170, 87–97.

Lin, Y.L., Farley, R.D., Orville, H.D., 1983. Bulk parameterization of the snow field in a cloud model. *J. Clim. Appl. Meteorol.* 22 (6), 1065–1092.

Liu, X.H., Zhang, Y., Cheng, S.H., Xing, J., Zhang, Q., Streets, D.G., et al., 2010a. Understanding of regional air pollution over China using CMAQ, part I performance evaluation and seasonal variation. *Atmos. Environ.* 44 (20), 2415–2426.

Liu, X.H., Zhang, Y., Xing, J., Zhang, Q., Wang, K., Streets, D.G., et al., 2010b. Understanding of regional air pollution over China using CMAQ, part II. Process analysis and sensitivity of ozone and particulate matter to precursor emissions. *Atmos. Environ.* 44 (30), 3719–3727.

Liu, X.G., Li, J., Qu, Y., Han, T., Hou, L., Gu, J., 2013. Formation and evolution mechanism of regional haze: A case study in the megacity Beijing, China. *Atmos. Chem. Phys.* 13 (9), 4501–4514.

Mlawer, E.J., Taubman, S.J., Brown, P.D., Lacono, M.J., Clough, S.A., 1997. Radiative transfer for inhomogeneous atmospheres: RRTM, a validated correlated-k model for the longwave. *J. Geophys. Res.* - Atmos. 102 (D14), 16663–16682.

Neumann, D., Matthias, V., Bieser, J., Aulinger, A., Quanté, M., 2016. Sensitivity of modeled atmospheric nitrogen species and nitrogen deposition to variations in sea salt emissions in the North Sea and Baltic Sea regions. *Atmos. Chem. Phys.* 16, 2921–2942.

Obukhov, A.M., 1971. Turbulence in an atmosphere with a non-uniform temperature. *Bound.-Layer Meteorol.* 2 (1), 7–29.

Qi, X.M., Ding, A.J., Nie, W., Petäjä, T., Kerminen, V.M., Herrmann, E., 2015. Aerosol size distribution and new particle formation in the western Yangtze River Delta of China. *Atmos. Chem. Phys.* 15 (21), 12445–12464.

- Quan, J., Zhang, Q., He, H., Liu, J., Huang, M., Jin, H., 2011. Analysis of the formation of fog and haze in North China Plain (NCP). *Atmos. Chem. Phys.* 11, 8205–8214.
- Quan, J., Tie, X.X., Zhang, Q., Liu, Q., Li, X., Gao, Y., et al., 2014. Characteristics of heavy aerosol pollution during the 2012–2013 winter in Beijing, China. *Atmos. Environ.* 88, 83–89.
- Sarwar, G., Luecken, D., 2008. Impact of an updated carbon bond mechanism on predictions from the CMAQ modeling system: Preliminary assessment. *J. Appl. Meteorol. Clim.* 47 (1), 7–12.
- Sun, Y.L., Zhuang, G.S., Tang, A.H., Wang, Y., An, Z.S., 2006. Chemical characteristics of  $PM_{2.5}$  and  $PM_{10}$  in haze-fog episodes in Beijing. *Environ. Sci. Technol.* 40, 3148–3155.
- Wang, J., Hu, Z.M., Chen, Y.Y., Chen, Z.L., Xu, S.Y., 2013. Contamination characteristics and possible sources of  $PM_{10}$  and  $PM_{2.5}$  in different functional areas of Shanghai, China. *Atmos. Environ.* 68 (2), 221–229.
- Wang, Y., Yao, L., Wang, L., Liu, Z., Ji, D., Tang, G., 2014a. Mechanism for the formation of the January 2013 heavy haze pollution episode over central and eastern China. *Sci. China: Earth Sci.* 57 (1), 14–25.
- Wang, J.D., Wang, S.X., Jiang, J.K., Ding, A.J., Zheng, M., Zhao, B., 2014b. Impact of aerosol–meteorology interactions on fine particle pollution during China’s severe haze episode in January 2013. *Environ. Res. Lett.* 9 (9), 094002.
- Wang, L.T., Wei, Z., Yang, J., Zhang, Y., Zhang, F.F., Su, J., et al., 2014c. The 2013 severe haze over the southern Hebei, China: model evaluation, source apportionment, and policy implications. *Atmos. Chem. Phys.* 14, 3151–3173.
- Wang, L.T., Wei, Z., Wei, W., Fu, J.S., Meng, C.C., Ma, S.M., 2015. Source apportionment of  $PM_{2.5}$  in top polluted cities in Hebei, China using the CMAQ model. *Atmos. Environ.* 122, 723–736.
- Xing, J., Zhang, Y., Wang, S.X., Liu, X.H., Cheng, S.H., Zhang, Q., 2011. Modeling study on the air quality impacts from emission reductions and atypical meteorological conditions during the 2008 Beijing Olympics. *Atmos. Environ.* 45, 1786–1798.
- Ye, X.N., Ma, Z., Zhang, J.C., Du, H.H., Chen, J.M., Chen, H., et al., 2011. Important role of ammonia on haze formation in Shanghai. *Environ. Res. Lett.* 6 (2), 024019.
- Zhang, Q., Quan, J.N., Tie, X.X., Li, X., Liu, Q., Gao, Y., et al., 2015. Effects of meteorology and secondary particle formation on visibility during heavy haze events in Beijing, China. *Sci. Total Environ.* 502, 578–584.
- Zhao, P.S., Dong, F., He, D., Zhao, X.J., Zhang, X.L., Zhang, W.Z., et al., 2013. Characteristics of concentrations and chemical compositions for  $PM_{2.5}$  in the region of Beijing, Tianjin, and Hebei, China. *Atmos. Chem. Phys.* 13, 4631–4644.
- Zhao, B., Wang, S.X., Xing, J., Fu, K., Fu, J.S., Jang, C., et al., 2015. Assessing the nonlinear response of fine particles to precursor emissions: development and application of an extended response surface modeling technique v1.0. *Geosci. Model Dev.* 8 (1), 115–128.
- Zheng, G.J., Duan, F.K., Su, H., Ma, Y.L., Cheng, Y., Zheng, B., et al., 2015. Exploring the severe winter haze in Beijing: the impact of synoptic weather, regional transport and heterogeneous reactions. *Atmos. Chem. Phys.* 15, 2969–2983.